Nnali-Uroh Emmanue, 2026, 14:4
ISSN (Online): 2348-4098
ISSN (Print): 2395-4752

International Journal of Science, Engineering and Technology
An Open Access Journal

Response Surface Methodology and Particle Swarm Optimization of Biodiesel Production from Waste Chicken Fat Oil Using KOH-Activated Chicken Bone Catalyst.

Nnali-Uroh Emmanue[1], Oluikpe Victor Amadi[2], Kolawole Idowu Sunday[3], Akpa Umahi Nwaeze[4]
[1,2,3,4]Advanced Unmanned Aerial Vehicle Laboratory (AUAVL), National Space Research and Development Agency (NASRDA) Abuja Nigeria

Abstract- This study investigates the optimization of biodiesel production from waste chicken fat oil using a KOH-activated chicken bone catalyst, employing an integrated experimental–computational approach. Response Surface Methodology (RSM), combined with Particle Swarm Optimization (PSO), was used to optimize five key process variables: catalyst dosage (0.5–2.5 wt%), reaction temperature (30–70 °C), reaction time (1–5 hours), methanol-to-oil ratio (6:1–14:1), and agitation speed (100–500 rpm). The optimal conditions predicted by RSM and PSO were: catalyst dosage of 1.30 wt%, methanol-to-oil ratio of 13.56:1, reaction time of 3.3 hours, and temperature of 77 °C. The resulting biodiesel yield was 97.42%, with a kinematic viscosity of 5.978 $mm^2 s^{-1}$ and a cetane index of 63.27, which meet the acceptable limits set by ASTM D6751 and EN 14214 standards. The study focused on the interactions of process variables, where the highest biodiesel yield was achieved by simultaneously increasing catalyst dosage and methanol ratio, with moderate temperature and extended reaction times. Statistical analysis using ANOVA revealed that the interaction model outperformed the linear model, with R^2 values of 0.6168 for biodiesel yield, 0.5233 for kinematic viscosity, and 0.5878 for cetane index, confirming the significance of interaction effects in the biodiesel production process. This research demonstrates that waste chicken fat oil, a low-cost feedstock, can be effectively utilized for biodiesel production. The optimized process conditions and integration of PSO for multi-response optimization provide a scalable and sustainable solution for biodiesel production from poultry-derived waste oils, contributing to waste-to-energy conversion

Keywords— Biodiesel Production, Waste Chicken Fat Oil, Particle Swarm Optimization (PSO), Response Surface Methodology (RSM), and KOH-Activated Chicken Bone Catalyst

I. INTRODUCTION

The urgent need for cleaner and sustainable energy sources has accelerated global interest in renewable transportation fuels (Singh et al., 2020). Biodiesel, a fuel composed of fatty acid alkyl esters, offers several advantages over petroleum diesel, including renewability, biodegradability, and compatibility with existing diesel engines. These attributes make biodiesel an important component of strategies aimed at reducing environmental pollution and dependence on fossil energy (Goh et al., 2019).

A major limitation to the broader deployment of biodiesel technology is production cost, which is largely controlled by the price and availability of feedstock (Rezania et al., 2019). Waste-derived lipids have therefore become attractive alternatives to edible oils. Waste chicken fat oil is generated in large quantities from poultry processing and represents an underutilized, low-cost resource for biodiesel production. However, animal fats are typically more viscous and compositionally variable than vegetable oils, making careful feedstock assessment essential prior to process optimization (Toldrá-Reig et al., 2020).

Reliable conversion of such feedstocks requires both effective catalysts and optimized operating conditions. Heterogeneous base catalysts produced from calcium-rich wastes have gained attention because they are inexpensive, reusable, and environmentally benign (Jayakumar et al., 2021). In this study, a KOH-activated chicken bone catalyst was employed as a practical solid catalyst for the transesterification of waste chicken fat oil. The objective of this work is not catalyst development or physicochemical characterization, but rather the systematic optimization of process conditions under which this catalyst can deliver maximum performance (Gupta et al., 2020).

Understanding the molecular composition of the feedstock is a critical step in biodiesel research. Techniques such as Fourier Transform Infrared Spectroscopy (FTIR) and Gas Chromatography–Mass Spectrometry (GC–MS) provide detailed information on functional groups and fatty acid profiles that influence reaction behavior and fuel quality (Karmakar & Halder, 2019). Accordingly, FTIR and GC–MS analyses were conducted in this study to evaluate the suitability of waste chicken fat oil for biodiesel production and to support subsequent process modeling (Athar & Zaidi, 2020)

Transesterification efficiency is affected by multiple interacting variables, including catalyst dosage, reaction temperature, reaction time, alcohol-to-oil ratio, and agitation intensity. Conventional one-factor-at-a-time experimentation is inadequate for such systems because it ignores interaction effects and often leads to suboptimal conditions (Tan et al., 2019). Response Surface Methodology (RSM) offers a structured statistical approach for evaluating multivariable processes with a limited number of experiments. Central Composite Design (CCD), a widely used RSM technique, enables the development of quadratic predictive models that accurately describe process behavior (Yusuff et al., 2021).

To further enhance optimization capability, intelligent computational algorithms can be integrated with RSM models. Particle Swarm Optimization (PSO) is a metaheuristic technique capable of locating global optima in complex nonlinear problems (Aghel et al., 2019). The combination of RSM and PSO provides a robust hybrid framework in which experimentally derived models serve as objective functions for multi-response optimization. This approach is particularly valuable for simultaneously improving biodiesel yield and key fuel properties such as kinematic viscosity and cetane index (Samuel et al., 2019).

The molecular structure of the feedstock was examined using Fourier Transform Infrared Spectroscopy. The FTIR spectrum revealed strong absorption bands near 1740 cm^{-1} corresponding to C=O ester stretching vibrations, confirming the triglyceride nature of the oil. Peaks observed around 2920 and 2850 cm^{-1} were attributed to aliphatic C–H stretching of long hydrocarbon chains, while bands near 1460 cm^{-1} indicated CH_2 bending vibrations (Nath et al., 2019). These characteristic signals verified that the waste chicken fat oil possessed the functional groups required for efficient transesterification (Falowo et al., 2020).

Gas Chromatography–Mass Spectrometry (GC–MS) analysis was conducted to determine the molecular composition of the waste chicken fat oil and to evaluate its suitability as a biodiesel feedstock. The complete chromatographic profile obtained from the analysis is presented in Figure 1. Although the chromatogram contains peaks from solvents and minor impurities, quantitative interpretation was restricted to compounds relevant to biodiesel production. Under the applied GC–MS conditions, fatty acids and fatty acid–related components eluted predominantly within the characteristic retention time range of 12–20 minutes. Peaks outside this region were therefore excluded from further evaluation (Adewale et al., 2019).

Analysis of the fatty acid region indicated that the feedstock consists mainly of long-chain C16 and C18 fatty acids. The processed compositional data derived from the chromatogram are summarized in Table 1. The results show a balanced distribution of saturated and monounsaturated fatty acids with a relatively low proportion of polyunsaturated components. The dominance of palmitic (C16:0) and

oleic (C18:1) acids is particularly beneficial, as these fatty acids are associated with improved cetane quality, good oxidative stability, and favorable viscosity characteristics (Kirubakaran & Arul Mozhi Selvan, 2018).

The novelty of this study lies in the integrated application of feedstock molecular characterization, five-factor Central Composite Design modeling, and Particle Swarm Optimization for biodiesel production from waste chicken fat oil using a KOH-activated chicken bone catalyst. Unlike most previous investigations that relied on one-factor-at-a-time experimentation or single-response optimization, this work simultaneously models and optimizes biodiesel yield, kinematic viscosity, and cetane index within a unified RSM–PSO framework. Furthermore, the study combines GC–MS and FTIR-based evaluation of the feedstock with advanced computational optimization to establish statistically validated operating conditions for a poultry-waste-based biodiesel system. To the best of our knowledge, such a comprehensive multi-response optimization approach for this specific feedstock–catalyst combination has not been previously reported.

This study aims to optimize biodiesel production from waste chicken fat oil using a KOH-activated chicken bone catalyst through an integrated experimental–computational approach. The specific objectives include characterizing waste chicken fat oil using FTIR and GC–MS to confirm its suitability as biodiesel feedstock, investigating the combined effects of five key process variables using a Central Composite Design, developing empirical predictive models for biodiesel yield, kinematic viscosity, and cetane index, evaluating the significance and interactions of process factors through ANOVA, and determining optimal operating conditions using Particle Swarm Optimization. By linking feedstock molecular evaluation with advanced statistical and computational optimization, this research provides a practical framework for efficient biodiesel production from poultry-derived wastes using a low-cost heterogeneous catalyst.

II. MATERIALS AND METHODS

1. Materials

Waste chicken fat was obtained from a local poultry processing facility and used as the primary lipid feedstock. Analytical-grade methanol (≥99.5% purity) and potassium hydroxide pellets were procured from standard chemical suppliers. Chicken bones used for catalyst preparation were collected from the same processing source to maintain material consistency. All reagents were used as received without further purification.

2. Feedstock Preparation

Chicken fat waste was sourced from the Abakaliki International Market in Ebonyi State, washed, and filtered to remove contaminants. Oil extraction was performed via wet rendering at 50°C for 20-25 minutes. The oil was characterized for physicochemical properties such as free fatty acid (FFA), moisture, viscosity, and other relevant parameters using GC-MS and FTIR. Standard analytical methods were followed to determine the moisture content, acid value, iodine value, peroxide value, saponification value, kinematic viscosity, specific gravity, refractive index, flash point, cloud point, pour point, smoke point, and boiling point in accordance with ASTM D6751 guidelines. FFA content was calculated using the acid value, and ester value and molecular weight were derived from saponification and acid values.

3. Catalyst Preparation

Alkaline Treatment and Calcination of Waste Chicken Bone

Chicken bones were sourced from Roban Stores, Abakaliki, washed thoroughly, and sun-dried until completely dried. The dried bones were ground using a local grinding machine and sieved to a particle size of 250 µm to ensure a consistent catalytic surface. The bones were then carbonized in a muffle furnace at 400, 600, 800, and 1000°C for 4 hours under an inert atmosphere. After calcination, the carbonized bones were washed with distilled water to remove impurities and neutralize the pH, followed by air-drying at room temperature. The resulting activated carbon (AC) was pulverized and stored in airtight containers. The AC yield was

calculated by comparing the post-activation weight to the initial sample weight using equation (1)

$$\% AC = \frac{\text{Weight of activated carbon}}{\text{Initial sample weight}} x\ 100 \quad (1)$$

Additionally, alkaline treatment was performed by refluxing the bones with a 2.5N NaOH solution at 100°C for 1.5 hours using a reflux system. The alkaline-impregnated catalyst was then filtered, dried, and calcined under similar conditions (400, 600, 800, and 1000°C for 4 hours in the absence of air), with yield calculations following the same equation.

Although advanced physicochemical characterization techniques such as XRD, SEM, and BET were not employed in this study, the catalytic performance was evaluated based on key reaction parameters, including biodiesel yield, reproducibility of the experimental runs, and the compliance of the produced fuel with ASTM D6751 and EN 14214 standards. This performance-based evaluation is a widely accepted approach for assessing waste-derived CaO-based heterogeneous catalysts, where functional catalytic activity and adherence to fuel standards are reliable indicators of the catalyst's suitability for biodiesel production. The use of functional evaluation methods has become increasingly common and well-supported in the literature concerning waste-based heterogeneous catalysts for biodiesel synthesis (Boro et al., 2012; Chouhan and Sarma, 2011; Birla et al., 2012).

Although advanced structural characterization techniques (XRD, SEM, BET) were not conducted in this study, catalyst performance was rigorously assessed through functional metrics, including biodiesel yield, experimental reproducibility across the CCD runs, and compliance with ASTM D6751 and EN 14214 standards. For waste-derived CaO heterogeneous catalysts, catalytic activity and the consistent production of standards-compliant biodiesel are widely accepted indicators of practical suitability in preliminary process optimization studies (Boro et al., 2012; Chouhan & Sarma, 2011; Birla et al., 2012). Nonetheless, structural and surface analyses remain essential for confirming phase composition, morphology, surface properties, and long-term stability. Accordingly, future work will incorporate XRD, SEM, BET, and catalyst reusability assessments to further validate catalyst integrity and durability under operational conditions.

4. FTIR Analysis of Waste Chicken Fat Oil

Fourier Transform Infrared Spectroscopy (FTIR) was used to identify functional groups present in the feedstock oil. Spectral analysis was performed using an FTIR spectrophotometer in the range of 4000–500 cm^{-1} with a resolution of 4 cm^{-1}. Samples were analyzed using the attenuated total reflectance (ATR) technique. The obtained spectra were examined to confirm the presence of characteristic triglyceride absorption bands and to evaluate structural features relevant to transesterification.

5. GC–MS Characterization

The fatty acid composition of the waste chicken fat oil was determined using Gas Chromatography–Mass Spectrometry (GC–MS). Prior to analysis, the oil sample was converted to fatty acid methyl esters (FAMEs) using standard derivatization procedures. The FAMEs were injected into the GC–MS system equipped with a capillary column and helium as the carrier gas. Individual fatty acids were identified by comparison with mass spectral libraries and retention times. The relative percentage composition of saturated and unsaturated fatty acids was calculated to assess feedstock suitability for biodiesel production.

6. Experimental Design Using Central Composite Design

Process optimization was carried out using Response Surface Methodology based on a five-factor Central Composite Design (CCD), where the independent variables investigated were catalyst dosage (A) ranging from 0.5 to 2.5 wt.%, reaction temperature (B) from 30 to 70 °C, reaction time (C) from 1 to 5 hours, methanol-to-oil molar ratio (D) from 6:1 to 14:1, and agitation speed (E) from 100 to 500 rpm, each studied at five coded levels ($-\alpha$, -1, 0, $+1$, $+\alpha$). A total of 32 experimental runs were generated, including factorial points, axial points, and replicated center points to estimate experimental error and model curvature, with biodiesel yield, kinematic viscosity, and cetane index selected as response

variables. All experiments were conducted according to the CCD matrix, and responses were recorded for subsequent modeling.

7. Transesterification Procedure

Biodiesel was produced via transesterification using heterogeneous catalysts in a three-neck round-bottom flask with a condenser, placed on a magnetic hot plate. Water circulated through the condenser to prevent evaporation. The study investigated five independent variables: catalyst dosage (A) from 0.5 to 2.5 wt.%, reaction temperature (B) from 30 to 70 °C, reaction time (C) from 1 to 5 hours, methanol-to-oil molar ratio (D) from 6:1 to 14:1, and agitation speed (E) from 100 to 500 rpm. The methanol-to-oil ratio was 12:1, and the catalyst concentration was 3% wt. of the oil. After each reaction, the mixture was transferred to a separating funnel and washed with boiling distilled water, causing methanol to evaporate. The biodiesel, being less dense than water, floated as the supernatant while impurities settled at the bottom. The water was drained, and the biodiesel was collected and dried in a water bath to remove excess water.

8. Determination of Response Variables

Biodiesel Yield

Biodiesel yield was calculated on a mass basis using the ratio of the weight of purified biodiesel obtained to the initial weight of oil used.

Kinematic Viscosity

The kinematic viscosity of the produced biodiesel was measured at 40 °C using a calibrated viscometer in accordance with ASTM standard procedures.

Cetane Index

Cetane index was estimated from measured fuel properties using established empirical correlations to evaluate ignition quality of the biodiesel samples.

9. RSM Modeling and Statistical Analysis

Experimental data obtained from the CCD runs were analyzed using Response Surface Methodology interactive polynomial models were developed to correlate the independent variables with each response. The general form of the model is:

$$Y = \beta_0 + \Sigma (\beta_i X_i) + \Sigma \Sigma (\beta_{ij} X_i X_j) + \varepsilon$$

where Y represents the predicted response, Xi and Xj are coded independent variables, and βi and βij terms are regression coefficients.

Model adequacy was evaluated using analysis of variance (ANOVA), coefficient of determination (R^2), adjusted R^2, and mean square error (MSE). The statistical significance of model terms was assessed at a 95% confidence level ($p < 0.05$). Diagnostic plots were used to verify model assumptions and goodness of fit.

10. Particle Swarm Optimization

Multi-objective optimization of the transesterification process was performed using Particle Swarm Optimization (PSO), with the RSM-derived regression equations for biodiesel yield, kinematic viscosity, and cetane index serving as objective functions in the PSO algorithm. The optimization goals were to maximize biodiesel yield, minimize kinematic viscosity, and maximize the cetane index. The PSO algorithm was implemented with the following settings: a population size of 30 particles, 50 maximum iterations, inertia weight of 0.7, cognitive coefficient of 1.5, and social coefficient of 1.5. The algorithm iteratively updated particle positions and velocities until convergence was achieved, and the optimal combination of process parameters predicted by PSO was compared with RSM-based optimal conditions to evaluate improvement in process performance.

11. Validation of Optimal Conditions

To assess the reliability of the optimization results, the adequacy of the models for biodiesel yield, kinematic viscosity, and cetane index was evaluated using key statistical indicators, including the coefficient of determination (R^2), adjusted R^2, and mean square error (MSE). These indicators helped verify the accuracy and practical applicability of the developed optimization framework

III. RESULTS AND DISCUSSION

1. FTIR Analysis of Waste Chicken Fat Oil

The molecular structure of the feedstock was examined using Fourier Transform Infrared Spectroscopy.

The FTIR spectrum (Figure 1) revealed strong absorption bands near 1740 cm^{-1} corresponding to C=O ester stretching vibrations, confirming the triglyceride nature of the oil. Peaks observed around 2920 and 2850 cm^{-1} were attributed to aliphatic C–H stretching of long hydrocarbon chains, while bands near 1460 cm^{-1} indicated CH_2 bending vibrations (Table 1). These characteristic signals verified that the waste chicken fat oil possessed the functional groups required for efficient transesterification (Nnali-Uroh et al., 2026; Kirubakaran & Selvan, 2018).

Table 1: Summary of key FTIR absorption bands of the waste chicken fat oil and the functional group identification.

Wavenumber (cm^{-1})	Functional group	Assignment
~3365	O–H stretching	Moisture / free fatty acids
2920	C–H stretching	Asymmetric $–CH_2$
2855	C–H stretching	Symmetric $–CH_2$
1742	C=O stretching	Ester carbonyl (triglycerides)
1462	C–H bending	$–CH_2$ scissoring
1371	C–H bending	$–CH_3$ bending
1155–1028	C–O stretching	Ester linkage
~721	$–(CH_2)_n$ rocking	Long-chain saturated fatty acids

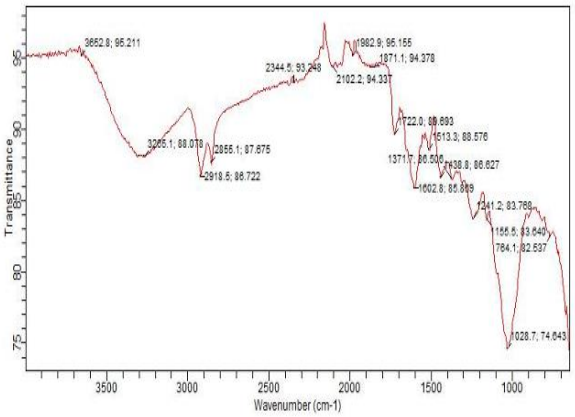

Figure 1. FTIR spectrum of waste chicken fat oil showing characteristic triglyceride functional groups.

2. GC–MS Characterization of Feedstock

Gas Chromatography–Mass Spectrometry (GC–MS) analysis was conducted to determine the molecular composition of the waste chicken fat oil and to evaluate its suitability as a biodiesel feedstock. The complete chromatographic profile obtained from the analysis is presented in Figure 2. Although the chromatogram contains peaks from solvents and minor impurities, quantitative interpretation was restricted to compounds relevant to biodiesel production. Analysis of the fatty acid region indicated that the feedstock consists mainly of long-chain C16 and C18 fatty acids. The processed compositional data derived from the chromatogram are summarized in Tables 2a and b . The results show a balanced distribution of saturated and monounsaturated fatty acids with a relatively low proportion of polyunsaturated components (Adewale et al., 2015). The dominance of palmitic (C16:0) and oleic (C18:1) acids is particularly beneficial, as these fatty acids are associated with improved cetane quality, good oxidative stability, and favorable viscosity characteristics (Kirubakaran & Selvan, 2018). These molecular features explain the desirable fuel properties observed in the optimized biodiesel reported in subsequent sections. Overall, the GC–MS findings confirm that waste chicken fat oil represents a suitable and sustainable non-edible feedstock for biodiesel production (Nnali-Uroh et al., 2026).

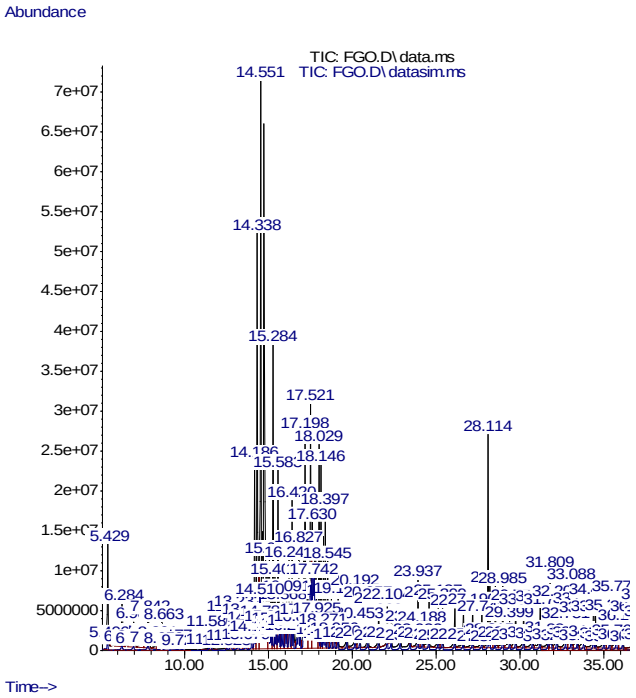

Figure 2. Total ion chromatogram (TIC) of waste chicken fat oil obtained from GC–MS analysis.

Table 2a. Fatty acid composition of waste chicken fat oil obtained from GC–MS analysis.

Fatty Acid Identified	Abbreviation	Carbon Structure	Type	Summed Area (%)
Palmitic acid	C16:0	Hexadecanoic acid	Saturated	25.03
Stearic acid	C18:0	Octadecanoic acid	Saturated	5.18
Oleic acid	C18:1	9-Octadecenoic acid	Monounsaturated	14.41
Palmitoleic acid	C16:1	9-Hexadecenoic acid	Monounsaturated	2.06
Vaccenic acid	C18:1	cis-11-Octadecenoic acid	Monounsaturated	11.10
Linoleic acid derivatives	C18:2	Octadecadienoic acid	Polyunsaturated	4.08
Minor fatty components	–	Various traces	Mixed	3.21
Total Identified Fatty Acids	–	–	–	65.07

Table 2b. Fatty Acid Class Distribution of waste chicken fat oil obtained from GC–MS analysis.

Fatty Acid Class	Total Percentage (%)
Saturated Fatty Acids (SFA)	30.21
Monounsaturated Fatty Acids (MUFA)	27.57
Polyunsaturated Fatty Acids (PUFA)	4.08

3. RSM Modeling and ANOVA Interpretation

RSM Modeling and Statistical Evaluation

The adequacy of the developed response surface models was assessed using analysis of variance for biodiesel yield, kinematic viscosity, and cetane index. For each response, both linear and interaction models were compared to determine the most appropriate representation of the experimental data.

Statistical Modeling of Biodiesel Yield

The comparative ANOVA results for biodiesel yield are summarized in Table 3a, which presents the performance of both the linear and interaction

models. The interaction model produced a higher coefficient of determination (R^2 = 0.6168) than the linear model (R^2 = 0.5423), indicating that inclusion of interaction and quadratic terms improved the predictive capability of the model (Dharma et al., 2016). These statistical results demonstrate that biodiesel yield is strongly affected by interactions among process variables such as catalyst dosage, methanol-to-oil ratio, temperature, and reaction time. The relatively lower adjusted R^2 value reflects the complexity of the five-factor system, but the model remains adequate for optimization within the experimental domain (Milano et al., 2018, Esonye et al, 2019).

The nature of these interactions is further illustrated using three-dimensional response surface plots shown in Figure 3a, b and c. The plots reveal that yield increased markedly with simultaneous increases in catalyst dosage and methanol ratio. Higher temperatures and longer reaction times also promoted improved conversion, confirming the multivariable dependence of the process (Ong et al., 2019).

Table 3a. Comparative ANOVA results for linear and interaction models of biodiesel yield

Model Type	R^2	Adjusted R^2	Mean Square Error (MSE)
Linear Model	0.5423	0.4542	97.1730
Interaction Model	0.6168	0.2603	131.7095

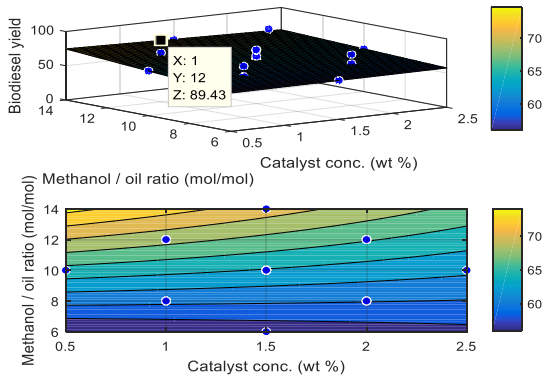

Figure 3a. Three-dimensional response surface plots illustrating the combined effects of process variables on biodiesel yield: (catalyst dosage and methanol-to-oil ratio)

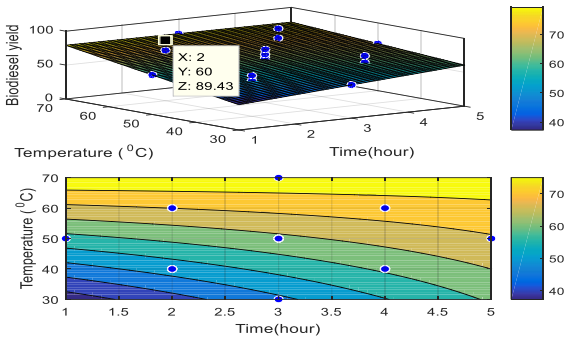

Figure 3b. Three-dimensional response surface plots illustrating the combined effects of process variables on biodiesel yield: (temperature and reaction time)

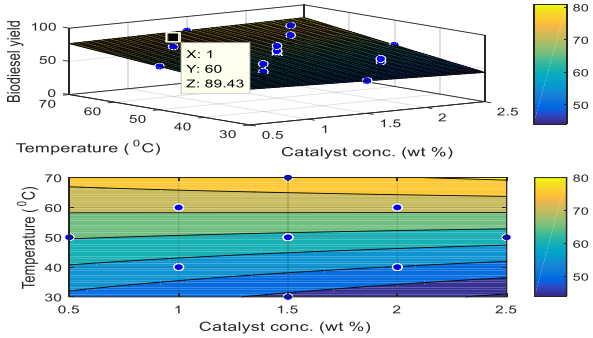

Figure 3c. Three-dimensional response surface plots illustrating the combined effects of process variables on biodiesel yield: (catalyst dosage and temperature)

Statistical Modeling of Kinematic Viscosity

Model performance for kinematic viscosity is presented in Table 3b. The interaction model (R^2 = 0.5233) provided a clear improvement over the linear model (R^2 = 0.3637), confirming that viscosity behavior depends on combined rather than isolated factor effects (Esonye et al., 2019). The ANOVA statistics indicate that temperature, reaction time, and catalyst dosage play significant roles in controlling viscosity. The inclusion of interaction terms substantially enhanced the model's descriptive power, validating the need for quadratic modeling (Sajjadi et al., 2016).

The influence of these parameters is visually represented in Figure 4a, b and c, where the surface plots show that viscosity decreased as reaction

temperature and time increased. Adequate agitation and catalyst concentration further contributed to viscosity reduction through improved mass transfer and reaction kinetics (Gülüm & Bilgin, 2017).

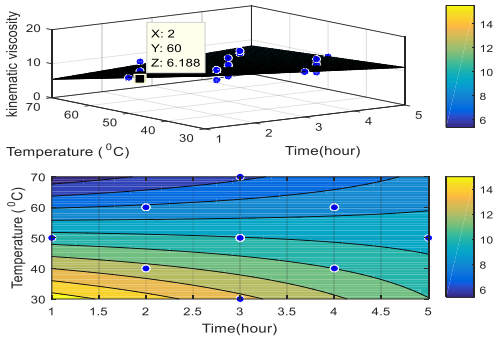

Figure 4a. Three-dimensional response surface plots showing the combined effects of process variables on kinematic viscosity (temperature and reaction time)

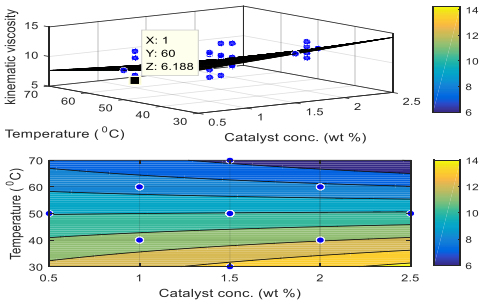

Figure 4b. Three-dimensional response surface plots showing the combined effects of process variables on kinematic viscosity: (catalyst dosage and temperature)

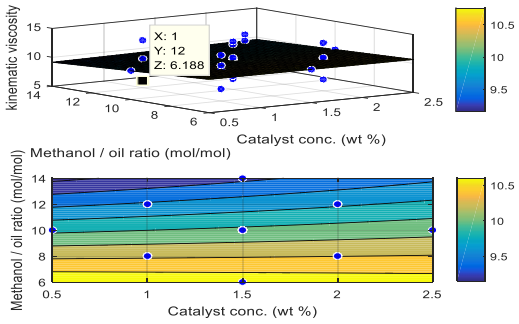

Figure 4c. Three-dimensional response surface plots showing the combined effects of process variables on kinematic viscosity: (methanol ratio and catalyst dosage).

Table 3b. Comparative ANOVA results for linear and interaction models of kinematic viscosity

Model Type	R^2	Adjusted R^2	Mean Square Error (MSE)
Linear Model	0.3637	0.4663	4.3639
Interaction Model	0.5233	0.0764	5.3344

Statistical Modeling of Cetane Index

The comparative ANOVA results for cetane index are provided in Table 3c. The interaction model achieved an R^2 value of 0.5878, outperforming the linear model (R^2 = 0.4892). This demonstrates that quadratic and interaction effects are essential for accurate prediction of cetane index (Onukwuli et al., 2017). Statistical analysis identified methanol-to-oil ratio and reaction temperature as the most influential variables affecting cetane index. The interaction effects observed confirm that ignition quality depends on balanced combinations of process conditions (Verma & Sharma, 2016).

These relationships are further clarified in Figure 5a, b and c, where the response surfaces show that moderate temperatures and higher methanol ratios favored higher cetane index values, reflecting improved ester conversion and fuel quality (Giakoumis & Sarakatsanis, 2019, Ofoefule et al, 2019).

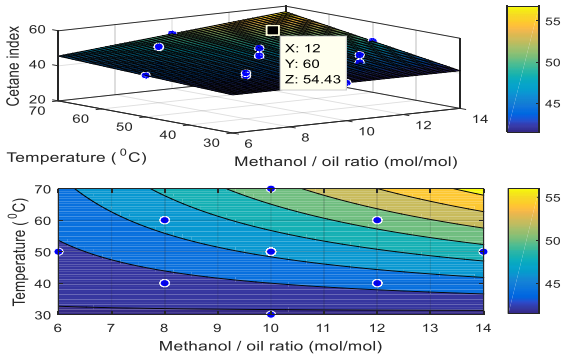

Figure 5a. Three-dimensional response surface plots illustrating the effects of process variables on cetane index: (methanol ratio and temperature).

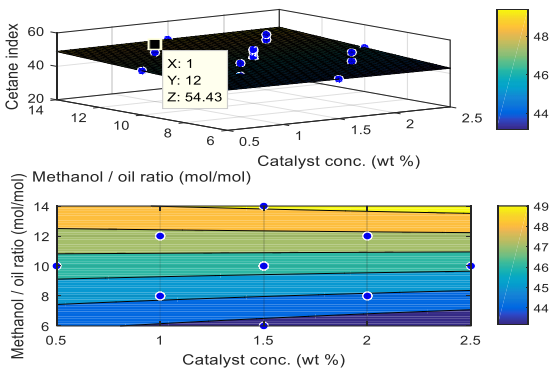

Figure 5b. Three-dimensional response surface plots illustrating the effects of process variables on cetane index: (catalyst dosage and methanol ratio)

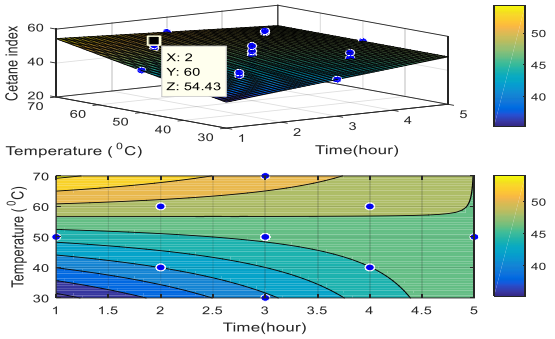

Figure 5c. Three-dimensional response surface plots illustrating the effects of process variables on cetane index: (temperature and reaction time).

Table 3c. Comparative ANOVA results for linear and interaction models of cetane index

Model Type	R^2	Adjusted R^2	Mean Square Error (MSE)
Linear Model	0.4892	0.3910	14.8104
Interaction Model	0.5878	0.2014	19.4212

4. Implications of ANOVA and Surface Plot Findings

The combined information from Tables 3a, b and c and Figures 3–5 confirms that the transesterification process is highly interactive and nonlinear. For all responses, interaction models consistently outperformed linear models, validating the application of Central Composite Design and multivariable optimization strategies.

5. Optimization Using RSM Desirability Approach

The optimal operating conditions predicted using classical RSM desirability analysis are summarized in Table 4a. Under these conditions—catalyst dosage of 1 wt%, methanol-to-oil ratio of 12:1, reaction time of 2 hours, temperature of 60 °C, and agitation speed of 400 rpm—the predicted responses were a biodiesel yield of 89.43%, a kinematic viscosity of 6.188 $mm^2 s^{-1}$, and a cetane index of 54.43 Table 4b, although further improvement was sought through advanced computational optimization (Milano et al., 2018).

Table 4a. Optimal operating conditions and predicted responses obtained from RSM desirability optimization

Parameter	Optimal Value
Catalyst dosage (wt%)	1.0
Methanol-to-oil molar ratio	12:1
Reaction time (h)	2.0
Reaction temperature (°C)	60
Agitation speed (rpm)	400

Table 4b. Predicted responses obtained from RSM desirability optimization

Response Variable	Predicted Value
Biodiesel yield (%)	89.43
Kinematic viscosity ($mm^2 s^{-1}$)	6.188
Cetane index	54.43

6. Multi-Objective Optimization Using Particle Swarm Optimization

The detailed iterative results obtained from Particle Swarm Optimization are presented in Table 5, which shows the progressive improvement of responses over successive iterations. The PSO algorithm identified the following optimal conditions: catalyst dosage of approximately 1.30 wt%, methanol-to-oil

ratio of 13.56:1, reaction time of 3.3 hours, temperature of 77 °C, and agitation speed of 442 rpm, resulting in optimized responses of a biodiesel yield of 97.42%, kinematic viscosity of 5.978 $mm^2 s^{-1}$, and a cetane index of 63.27 (Aghbashlo et al., 2021). The convergence behavior of the algorithm is illustrated in Figure 6a, b and c, demonstrating stable and consistent movement toward optimal solutions (Esonye et al., 2019).

Table 5. Iterative results of Particle Swarm Optimization showing progressive improvement of process responses

Iteratio	Catalyst dosage	Methanol/Oil	Time (h)	Temp	Speed (rpm)	Yield (%)	Viscosity ($mm^2 s^{-1}$)	Cetane Index
1	1.00	12.00	2.0	60	400	89.43	6.1879	54.43
2	1.01	12.00	2.0	60	400	89.92	6.1792	55.21
3	1.05	12.00	2.0	60	400	90.54	6.1786	55.34
4	1.12	12.00	2.0	60	400	90.58	6.1780	55.38
5	1.16	12.00	2.0	60	400	90.60	6.1779	55.40
6	1.23	12.00	2.0	60	400	90.60	6.1779	55.41
7	1.30	12.00	2.0	60	400	90.60	6.1779	55.41
8	1.30	12.13	2.0	60	400	91.47	6.1586	57.01
9	1.30	12.19	2.0	60	400	91.88	6.1492	57.67
10	1.30	12.36	2.0	60	400	91.97	6.1487	57.77
11	1.30	12.67	2.0	60	400	92.02	6.1483	57.82
12	1.30	12.98	2.0	60	400	92.05	6.1482	57.85
13	1.30	13.11	2.0	60	400	92.02	6.1482	57.87
14	1.30	13.56	2.0	60	400	92.02	6.1482	57.87
15	1.30	13.56	2.1	60	400	94.17	6.1217	58.98
16	1.30	13.56	2.3	60	400	94.83	6.1182	59.13
17	1.30	13.56	2.6	60	400	94.99	6.1173	59.21
18	1.30	13.56	2.9	60	400	95.05	6.1170	59.27
19	1.30	13.56	3.1	60	400	95.05	6.1170	59.34
20	1.30	13.56	3.3	60	400	95.05	6.1170	59.34
21	1.30	13.56	3.3	62	400	96.89	6.0092	61.33
22	1.30	13.56	3.3	65	400	96.95	6.0011	61.73
23	1.30	13.56	3.3	67	400	96.93	5.9997	61.81
24	1.30	13.56	3.3	70	400	96.91	5.9993	61.84
25	1.30	13.56	3.3	74	400	96.91	5.9991	61.86
26	1.30	13.56	3.3	77	400	96.91	5.9991	61.88
27	1.30	13.56	3.3	77	405	97.21	5.9884	63.01
28	1.30	13.56	3.3	77	411	97.34	5.9795	63.17
29	1.30	13.56	3.3	77	417	97.38	5.9787	63.21
30	1.30	13.56	3.3	77	421	97.41	5.9783	63.25
31	1.30	13.56	3.3	77	431	97.42	5.9780	63.27
32	1.30	13.56	3.3	77	442	97.42	5.9780	63.27

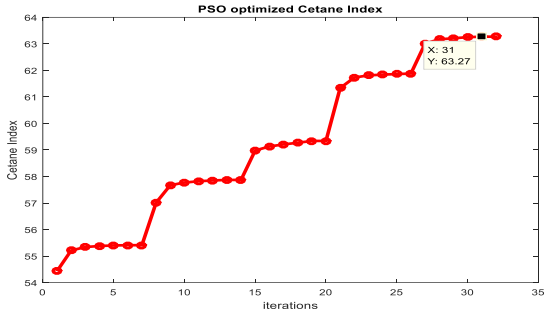

Figure 6a. Convergence profile of Particle Swarm Optimization for Biodiesel yield

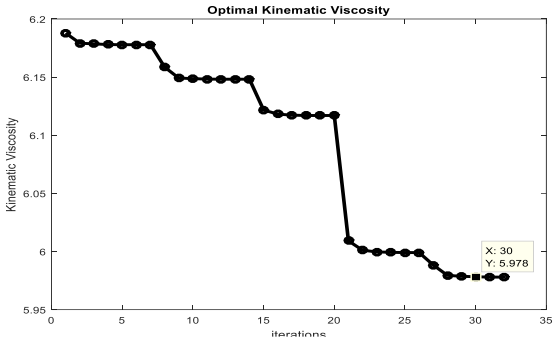

Figure 6b. Convergence profile of Particle Swarm Optimization for kinematic Viscosity.

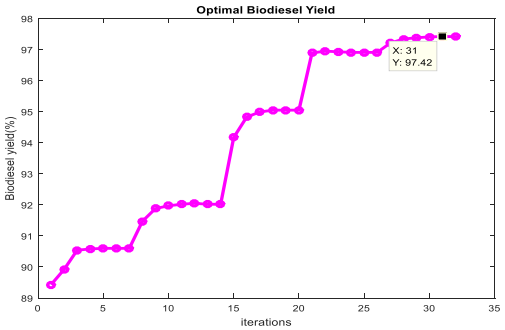

Figure 6c. Convergence profile of Particle Swarm Optimization for Cetane index

7. Comparative Evaluation of RSM and PSO Optimization

The comparison clearly shows that PSO optimization delivered superior results, increasing yield by approximately 8%, reducing viscosity to more desirable values, and significantly enhancing cetane index. These improvements demonstrate the advantage of integrating RSM modeling with intelligent optimization techniques (Esonye et al, 2023; Ishola et al., 2019). A direct comparison of the two optimization approaches is provided in Table 6.

Table 6. Comparison of optimal responses obtained from RSM and PSO optimization methods

Optimization Method	Catalyst Dosage (wt%)	Methanol/Oil Ratio	Time (h)	Temperature (°C)	Agitation Speed (rpm)	Biodiesel Yield (%)	Kinematic Viscosity ($mm^2 s^{-1}$)	Cetane Index
RSM Desirability	1.0	12:1	2.0	60	400	89.43	6.188	54.43
PSO Optimization	1.30	13.56:1	3.3	77	442	97.42	5.978	63.27

8. Model Adequacy Validation

The reliability of the optimization results was validated through a thorough statistical evaluation of the RSM models. Key indicators, including R^2, adjusted R^2, and mean square error (MSE), were used to assess model performance for biodiesel yield, kinematic viscosity, and cetane index, as shown in

Table 7. The R^2 values indicated a strong correlation between the models and the experimental data, although adjusted R^2 values were lower due to the complexity of the five-factor design (Hamze et al., 2015). Despite this, the models remained statistically valid and predictive. The low MSE values further confirmed the models' accuracy (Razavi et al., 2019).

Additionally, the close alignment between RSM-predicted and PSO-optimized results, with the PSO algorithm converging towards improved solutions, reinforces the models' reliability.

Overall, the combination of robust goodness-of-fit statistics and consistent optimization results supports the use of the RSM–PSO framework for process optimization, with future experimental validation recommended at the predicted optimum (Ajala et al., 2020).

Table 7. Statistical adequacy indicators for developed RSM models

Response Variable	R^2	Adjusted R^2	Mean Square Error (MSE)
Biodiesel yield	0.6168	0.2603	131.7095
Kinematic viscosity	0.5233	0.0764	5.3344
Cetane index	0.5878	0.2014	19.4212

9. Fuel Quality Compliance Assessment

The fuel quality of the biodiesel produced under PSO-optimized conditions was evaluated against international biodiesel standards. As shown in Table 8, the kinematic viscosity of 5.978 $mm^2 s^{-1}$ falls within the acceptable range specified by ASTM D6751 (1.9–6.0 $mm^2 s^{-1}$), confirming suitability for diesel engine applications.

Although slightly above the stricter EN 14214 upper limit of 5.0 $mm^2 s^{-1}$, the value remains within widely accepted ASTM requirements (Silitonga et al., 2016).

The cetane index of 63.27 significantly exceeds the minimum requirements of both ASTM D6751 (≥47) and EN 14214 (≥51), indicating excellent ignition quality and combustion performance.

These results demonstrate that biodiesel produced from waste chicken fat oil using the optimized process conditions possesses fuel properties that

meet major international standards (Kirubakaran & Selvan, 2018).

Table 8. Comparison of optimized biodiesel fuel properties with ASTM D6751 and EN 14214 standards

Property	Unit	This Study (PSO Optimized)	ASTM D6751 Limit	EN 14214 Limit	Compliance
Kinematic viscosity @40 °C	$mm^2 s^{-1}$	5.978	1.9 – 6.0	3.5 – 5.0	ASTM: Compliant
Cetane index	–	63.27	≥ 47	≥ 51	Compliant
Biodiesel yield	%	97.42	–	–	–
Density (typical range)*	$kg\ m^{-3}$	Within biodiesel range	–	860 – 900	Expected
Acid value*	mg KOH g^{-1}	Within acceptable range	≤ 0.50	≤ 0.50	Expected

IV. CONCLUSION

This study successfully optimized biodiesel production from waste chicken fat oil using a KOH-activated chicken bone catalyst, employing a novel combination of Response Surface Methodology (RSM) and Particle Swarm Optimization (PSO). The integration of feedstock molecular characterization with advanced statistical and computational optimization techniques resulted in a robust framework that enhances biodiesel yield, viscosity, and cetane index. Through systematic process modeling, we identified optimal conditions—catalyst dosage of 1.30 wt%, methanol-to-oil ratio of 13.56:1, reaction time of 3.3 hours, and temperature of 77°C—that significantly improved the fuel properties compared to conventional optimization methods.

The findings highlight the substantial potential of utilizing waste-derived lipids, particularly waste chicken fat oil, as an economical and sustainable feedstock for biodiesel production. The optimized biodiesel met the international standards set by ASTM D6751 and EN 14214, demonstrating its suitability for diesel engine applications. This work underscores the importance of integrating computational optimization techniques such as PSO with traditional RSM to achieve superior biodiesel quality and process efficiency.

Future research should focus on experimental validation of the predicted conditions, further refining the optimization framework for commercial-scale biodiesel production from poultry waste. This approach provides a sustainable, cost-effective solution for the biodiesel industry and contributes to the ongoing efforts to reduce dependence on fossil fuels and mitigate environmental pollution.

REFERENCE

1. Adewale, P., Dumont, M.-J., & Ngadi, M. (2019). Enzyme-catalyzed synthesis and kinetics of ultrasonic-assisted biodiesel production from waste tallow. Ultrasonics Sonochemistry, 51, 347–355. https://doi.org/10.1016/j.ultsonch.2018.10.028
2. Aghbashlo, M., Peng, W., Tabatabaei, M., Kalogirou, S.A., Soltanian, S., Hosseinzadeh-Bandbafha, H., Mahian, O., and Lam, S.S. (2021). Machine learning technology in biodiesel research: A review. Progress in Energy and Combustion Science, 85, 100904.
3. Aghel, B., Mohadesi, M., Sahraei, S., & Shariatifar, M. (2019). New heterogeneous process for biodiesel production from waste cooking oil using particle swarm optimization and response surface methodology. Waste Management, 93, 59–67. https://doi.org/10.1016/j.wasman.2019.05.029
4. Ajala, E.O., Ajala, M.A., Ayinla, I.K., Sonusi, A.D., and Fanodun, S.E. (2020). Nano-synthesis of solid acid catalysts from waste-iron-filling for biodiesel production using high free fatty acid waste cooking oil. Scientific Reports, 10, 13256.

5. Alptekin, E., Canakci, M., Ozsezen, A.N., Turkcan, A., & Sanli, H. (2020). Using waste animal fat based biodiesels–bioethanol–diesel fuel blends in a DI diesel engine. Fuel, 255, 115794. https://doi.org/10.1016/j.fuel.2019.115794
6. Anderson, M.J., & Whitcomb, P.J. (2016). RSM Simplified: Optimizing Processes Using Response Surface Methods for Design of Experiments (2nd ed.). CRC Press. https://doi.org/10.1201/9781315382326
7. Athar, M., & Zaidi, S. (2020). A review of the feedstocks, catalysts, and intensification techniques for sustainable biodiesel production. Journal of Environmental Chemical Engineering, 8(6), 104523. https://doi.org/10.1016/j.jece.2020.104523
8. Ayoub, M., Putra, M.D., Ullah, S., Ahmad, M., Sultana, S., & Zahid, I. (2019). Comprehensive study on biodiesel production from waste cooking oil using K2CO3 impregnated calcined clam shell as heterogeneous catalyst. Energy Conversion and Management, 195, 1103–1117. https://doi.org/10.1016/j.enconman.2019.05.096
9. Birla, A., Singh, B., Upadhyay, S. N., & Sharma, Y. C. (2012). Kinetic studies of biodiesel synthesis from waste frying oil using a heterogeneous catalyst derived from snail shell. Bioresource Technology, 106, 95–100. https://doi.org/10.1016/j.biortech.2011.11.065
10. Birla, A., Singh, B., Upadhyay, S. N., & Sharma, Y. C. (2012). Kinetic studies of biodiesel synthesis from waste frying oil using a heterogeneous catalyst derived from snail shell. Bioresource Technology, 106, 95–100. https://doi.org/10.1016/j.biortech.2011.11.065
11. Boro, J., Deka, D., & Thakur, A. J. (2012). A review on solid oxide derived from waste shells as catalyst for biodiesel production. Renewable and Sustainable Energy Reviews, 16(1), 904–910. https://doi.org/10.1016/j.rser.2011.09.011
12. Boro, J., Deka, D., & Thakur, A. J. (2012). A review on solid oxide derived from waste shells as catalyst for biodiesel production. Renewable and Sustainable Energy Reviews, 16(1), 904–910. https://doi.org/10.1016/j.rser.2011.09.011
13. Chouhan, A. P. S., & Sarma, A. K. (2011). Modern heterogeneous catalysts for biodiesel production: A comprehensive review. Renewable and Sustainable Energy Reviews, 15(9), 4378–4399. https://doi.org/10.1016/j.rser.2011.07.112
14. Chouhan, A. P. S., & Sarma, A. K. (2011). Modern heterogeneous catalysts for biodiesel production: A comprehensive review. Renewable and Sustainable Energy Reviews, 15(9), 4378–4399. https://doi.org/10.1016/j.rser.2011.07.112
15. Dharma, S., Masjuki, H.H., Hwai Ong, H., Sebayang, A.H., Silitonga, A.S., Kusumo, F., & Mahlia, T.M.I. (2016). Optimization of biodiesel production process for mixed Jatropha curcas–Ceiba pentandra biodiesel using response surface methodology. Energy Conversion and Management, 115, 178–190. https://doi.org/10.1016/j.enconman.2016.02.034
16. Esonye, C., Onukwuli, O. D. and Ofoefule, A. U. (2019). Optimization of Methyl Ester Production from Prunus Amygdalus Seed Oil Using Response Surface Methodology and Artificial Neural Networks. Renewable Energy, 130, 62-71,http://dx.doi.org/10.1016/j.renene.2018.06.036.
17. Esonye, C., Onukwuli, O. D., Okolie C. U. Anietie, O. E., Ume, C. S And Agu, C. M. (2023). Recursive Neural Network-Particle Swarm versus Non-Linear Multivariate Rational Function Algorithms for Optimization of Biodiesel Derived From Havea Brasiliences. Arabian Journal for Science and Engineering. 48: 15979-15998 https://doi.org/10.1007/s13369-023-07947-x.
18. Esonye, C., Onukwuli, O.D., and Ofoefule, A.U. (2019). Optimization of the methanolysis of lard oil in the production of biodiesel with response surface methodology. Egyptian Journal of Petroleum, 28(2), 149–157.
19. Falowo, O.A., Oloko-Oba, M.I., & Betiku, E. (2020). Biodiesel production intensification via microwave irradiation-assisted transesterification of oil blend using nanoparticles from elephant-ear tree pod husk as a base heterogeneous catalyst. Chemical Engineering and Processing – Process Intensification, 153, 107987. https://doi.org/10.1016/j.cep.2020.107987
20. Giakoumis, E.G., and Sarakatsanis, C.K. (2019). A comparative assessment of biodiesel cetane

number predictive correlations based on fatty acid composition. Energies, 12(3), 422.
21. Goh, B.H.H., Ong, H.C., Cheah, M.Y., Chen, W.H., Yu, K.L., & Mahlia, T.M.I. (2019). Sustainability of direct biodiesel synthesis from microalgae biomass: A critical review. Renewable and Sustainable Energy Reviews, 107, 59–74. https://doi.org/10.1016/j.rser.2019.02.012
22. Gülüm, M., and Bilgin, A. (2017). Two-term power models for estimating kinematic viscosities of different biodiesel-diesel fuel blends. Fuel Processing Technology, 149, 121–130.
23. Gupta, J., Agarwal, M., & Dalai, A.K. (2020). An overview on the recent advancements of sustainable heterogeneous catalysts and prominent continuous reactor for biodiesel production. Journal of Industrial and Engineering Chemistry, 88, 58–77. https://doi.org/10.1016/j.jiec.2020.05.012
24. Hamze, H., Akia, M., and Yazdani, F. (2015). Optimization of biodiesel production from the waste cooking oil using response surface methodology. Process Safety and Environmental Protection, 94, 1–10.
25. Ishola, N.B., Adeyemi, O.O., Adesina, A.J., Odude, V.O., Oyetunde, O.O., and Betiku, E. (2019). Process modeling and optimization of sorrel biodiesel synthesis using barium hydroxide as a base heterogeneous catalyst: Appraisal of response surface methodology, neural network and neuro-fuzzy system. Neural Computing and Applications, 31, 4929–4943.
26. Jayakumar, M., Karmegam, N., Gundupalli, M.P., Gebeyehu, K.B., Asfaw, B.T., Chang, S.W., Ravindran, B., & Awasthi, M.K. (2021). Heterogeneous base catalysts: Synthesis and application for biodiesel production – A review. Bioresource Technology, 331, 125054. https://doi.org/10.1016/j.biortech.2021.125054
27. Karmakar, B., & Halder, G. (2019). Progress and future of biodiesel synthesis: Advancements in oil extraction and conversion technologies. Energy Conversion and Management, 182, 307–339. https://doi.org/10.1016/j.enconman.2018.12.066
28. Kirubakaran, M., & Arul Mozhi Selvan, V. (2018). A comprehensive review of low cost biodiesel production from waste chicken fat. Renewable and Sustainable Energy Reviews, 82, 390–401. https://doi.org/10.1016/j.rser.2017.09.039
29. Milano, J., Ong, H.C., Masjuki, H.H., Silitonga, A.S., Chen, W.H., Kusumo, F., Dharma, S., and Sebayang, A.H. (2018). Optimization of biodiesel production by microwave irradiation-assisted transesterification for waste cooking oil-Calophyllum inophyllum oil via response surface methodology. Energy Conversion and Management, 158, 400-415.
30. Nath, B., Das, B., Kalita, P., & Basumatary, S. (2019). Waste to value addition: Utilization of waste Brassica nigra plant derived novel green heterogeneous base catalyst for effective synthesis of biodiesel. Journal of Cleaner Production, 239, 118112. https://doi.org/10.1016/j.jclepro.2019.118112
31. Nnali-Uroh E, Amaechi, E. T., Chizoo, E., Onukwuli, D. O., Menkiti, M., Amadi, O. V., Ikechukwu, N., & Oyinkro, A. N. (2026). Biodiesel Production from Waste Chicken Fat Oil Using a KOH- Activated Chicken Bone Catalyst. 3(1). https://doi.org/10.5281/zenodo.18605623
32. Ofoefule, A. U., Esonye, C. Onukwuli, O. D., Nwaeze, E., Ume, C. S.(2019) Modeling and optimization of African pear seed oil esterification and transesterification using artificial neural network and response surface methodology comparative analysis. Industrial Crops & Products, 140 111707 https://doi.org/10.1016/j.indcrop.2019.111707. Elsevier publications.
33. Ong, H.C., Milano, J., Silitonga, A.S., Hassan, M.H., Shamsuddin, A.H., Wang, C.T., Mahlia, T.M.I., Siswantoro, J., Kusumo, F., and Sutrisno, J. (2019). Biodiesel production from Calophyllum inophyllum-Ceiba pentandra oil mixture: Optimization and characterization. Journal of Cleaner Production, 219, 183-198.
34. Onukwuli, D.O., Emembolu, L.N., Ude, C.N., Aliozo, S.O., and Menkiti, M.C. (2017). Optimization of biodiesel production from refined cotton seed oil and its characterization. Egyptian Journal of Petroleum, 26(1), 103–110.

35. Razavi, R., Bemani, A., Baghban, A., Mohammadi, A.H., and Habibzadeh, S. (2019). An insight into the estimation of fatty acid methyl ester based biodiesel properties using a LSSVM model. Fuel, 243, 133–141.
36. Rezania, S., Oryani, B., Park, J., Hashemi, B., Yadav, K.K., Kwon, E.E., Hur, J., & Cho, J. (2019). Review on transesterification of non-edible sources for biodiesel production with a focus on economic aspects, fuel properties and by-product applications. Energy Conversion and Management, 201, 112155. https://doi.org/10.1016/j.enconman.2019.112155
37. Sajjadi, B., Raman, A.A.A., and Arandiyan, H. (2016). A comprehensive review on properties of edible and non-edible vegetable oil-based biodiesel: Composition, specifications and prediction models. Renewable and Sustainable Energy Reviews, 63, 62–92.
38. Samuel, O.D., Okwu, M.O., Oyejide, O.J., Taghinezhad, E., Afzal, A., & Kaveh, M. (2019). Optimizing biodiesel production from abundant waste oils through empirical method and grey wolf optimizer. Fuel, 281, 118701. https://doi.org/10.1016/j.fuel.2020.118701
39. Silitonga, A.S., Masjuki, H.H., Ong, H.C., Sebayang, A.H., Dharma, S., Kusumo, F., Siswantoro, J., Milano, J., Daud, K., Mahlia, T.M.I., Chen, W.H., and Sugiyanto, B. (2016). Evaluation of the engine performance and exhaust emissions of biodiesel-bioethanol-diesel blends using kernel-based extreme learning machine. Energy, 111, 1089–1103.
40. Singh, D., Sharma, D., Soni, S.L., Sharma, S., Sharma, P.K., & Jhalani, A. (2020). A review on feedstocks, production processes, and yield for different generations of biodiesel. Fuel, 262, 116553. https://doi.org/10.1016/j.fuel.2019.116553
41. Toldrá-Reig, F., Mora, L., & Toldrá, F. (2020). Trends in biodiesel production from animal fat waste. Applied Sciences, 10(10), 3644. https://doi.org/10.3390/app10103644
42. Verma, P., and Sharma, M.P. (2016). Review of process parameters for biodiesel production from different feedstocks. Renewable and Sustainable Energy Reviews, 62, 1063–1071.
43. Yusuff, A.S., Bhonsle, A.K., Trivedi, J., Kaushik, N., Bhan, C., & Shukla, A.K. (2021). Optimization and mechanism of biodiesel production from a novel heterogeneous cattle bone-derived catalyst. Fuel, 288, 119642. https://doi.org/10.1016/j.fuel.2020.119642